GPR Journals
www.gprjournals.org

Journal of Environmental and Geographical Studies
ISSN 2958 - 4116 (Online)
Vol.2, Issue 1, pp 1 – 24, 2023

Atmospheric Correction of Landsat Image

Jonah Iyowuna Benjamin[1*] and Aketi Taripredo Moses[2]

[1]Department of Surveying and Geomatics, Rivers State University, Port Harcourt.

[2]Nigeria Maritime University, Okerenkoko, Gbaramatu, Delta State

[*]Corresponding Author's Email: iyowunajs@gmail.com

Article History

Submitted: 18th Dec 2022
Accepted: 4th Feb 2023
Published: 24th Feb 2023

Abstract

Purpose: The satellite imagery such as Landsat contains water vapour and gases that do interfere with analytical process to lower the result. The research focused on atmospheric corrected and un-corrected image on Normalized Difference Vegetation Index determination. The aim of the paper was atmospheric correction on satellite imagery and the objectives considered were to: (1) discuss the types of atmospheric correction (2) determine the Normalized Difference Vegetation Index using atmospheric corrected image (3) highlight the Normalized Difference Vegetation Index without atmospheric corrected image.

Methodology: The following materials were used for the study, they are Landsat imagery, ArcGIS 10.7 and Idrisi 32 software. Remote sensing and Geographical Information Systems (GIS), were factored in the process of Normalize Difference Vegetation Index (NDVI) determination using bands 4 and 3. Additive rescaling formular was used to extract the temperature values. Analysis of variance was also conducted on the two NDVIs and presented in regression table.

Findings: The study found that atmospheric corrected NDVI started from 0.02 to 1.0 on the scale of measurement while uncorrected NDVI ranges from <61.00 to 201.

Conclusion: The study conclude that corrected satellite imagery gave a good reflectance of the earth features than uncorrected image.

Recommendation: The study recommend that for image studies to be carried out, there should be an atmospheric correction to have a precise result.

Keywords: *Atmospheric correction, NDVI, temperature*

GPR Journals
www.gprjournals.org
Journal of Environmental and Geographical Studies
ISSN 2958 - 4116 (Online)
Vol.2, Issue 1, pp 1 – 24, 2023

1.0 INTRODUCTION

Satellite observation is becoming a daily need as a result of its importance in the event of environmental monitoring. Remotely sensed imagery has been used for developing and validating various studies regarding land cover dynamics such as global carbon modelling, biogeochemical cycling, hydrological modelling, and ecosystem response modelling (Fallah et al., 1995). Various objects are recorded by the sensor based on their reflective value to make real time quantitative measurement. For this process to be real, atmospheric correction need to be accounted for. That is to say that gaseous absorption and scattering by molecules and aerosols and the sun-target-sensor geometry, and the surface characteristics need, also to be considered in order to obtain accurate surface reflectance values (Teillet, 1992; Tanré et al., 1992). International Institute for Geo-Information Science and Earth Observation (2004) better stated it that the atmosphere is a combination of water vapour, aerosols and gaseous particles which perturb the signal reaching the sensor in many ways. It would therefore, be necessary to make atmospheric correction to clean the images from these disturbances to allow pure ground radiance from the target (Holben et al., 1992; Holben et al., 1998, Kaufman et al., 1997).

Research have shown that atmospheric correction is a complex exercise considering the temporal and spatial nature of the satellite. For instance, radiative transfer in the atmosphere must be well understood in the actual implementation. In the circumstances of this, several methodologies have been developed to remove the effect of the atmosphere on the recorded satellite signal and these are Radiative Transfer Codes (RTC) have been widely used by the remote sensing community for this purpose, such as the 6S code (Second Simulation of the Satellite Signal in the Solar Spectrum and MODTRAN (Berk et al., 1989; Vermote et al., 1997a; Moran et al., 2001; Teillet & Fedosejevs, 1995; Gilabert et al., 1994; Rahman & Dedieu, 1994; Kneizys et al., 1988).

Literature studies further indicated other pertinent methods for removing atmospheric effects. These methods not only vary but transformed the direct digital number (DN) of image – dark object subtraction of atmospheric radiance path and cosine estimation of atmospheric transmittance (Caselles & Garcia, 1989; Smith &Milton, 1999; Chavez, 1988; 1996; Vincent, 1972). Dark object subtraction (DOS) is a model which shows zero reflectance with respect to assumption of dark object within an image (Gilabert et al., 1994; Moran et al., 1992; Chavez, 1996). They said that atmospheric radiance path is a function of corresponding pixels which invariably cause atmospheric scattering. Thus, each pixel selected from the histogram methods are subtracted from all selective values across the image. The cosine is developed based on multiplicative event of atmospheric scattering and absorption. Solar Zenith angle or satellite view angle (h) is used to approximate atmospheric transmittance (Thk).

Song et al., (2001) asserted the effectiveness of seven absolute atmospheric correction algorithms based upon the darkest pixel (DP) principle and one relative atmospheric correction, the multi-temporal normalization method by using stable features in the scene. They based their classification on change detection principles applied on a multi-temporal dataset of seven Landsat-5 TM images. Their results certified best by combining both atmospheric models and the dark object concept. Hadjimitsis et al., (2004) in their research work used DP method to evaluate the effectiveness of Landsat TM images over water treatment reservoirs, image-based atmospheric correction algorithms and other algorithms that make use of atmospheric modelling. Result was excellent for Landsat TM visible bands and Chrysoulakis et al., (2010) also reported the same their study using ASTHER data.

GPR Journals
www.gprjournals.org
Journal of Environmental and Geographical Studies
ISSN 2958 - 4116 (Online)
Vol.2, Issue 1, pp 1 – 24, 2023

More so, tabular method is another good way of eliminating atmospheric effect where look up tables were created to performed comparative analysis of Landsat TM, AVIRIS and other imaging spectrometer, results showed relative high accuracy (Fraser et al., 1992; Richer, 1990; Staenz &Williams, 1997; Moran et al., 1992; Farrand et al.,1994; ferrier, 1995; Dwyer et al., 1995). Song et al. (2001) is also lamented about the computational profile of the said correction which is cumbersome because its involvement in pixel by pixel correction, which would be too large for satellite image of large curvature. Beside this method, there is another aspect called the point spread function recommended by National Agency for Space Administration (NASA), fund collaborated with NSF long term Ecological Research (LTER) for site network on atmospheric correction revalidation duly developed by (Quaidrari & Vermote, 1999). This technique was applied to Landsat Thematic Mapper (TM) at 30 meters resolution up to a distance of 20 pixels around a viewed pixel over a processing time.

Running et al. (1994) tested MODLAND validation sites where Sun photometer data were collected at these sites contemporaneously with the satellite data. Using these data, atmospheric correction over the sites as well as the aerosol product which was used as input to the atmospheric correction (MODIS Land Aerosol ATBD). Roger et al. (1994) took a step further to use pre-launch validation with a high-altitude airborne data from the MODIS Airborne Simulator (MAS) collected during specific validation campaigns such as the Sulphate Cloud Aerosol Reflectance-Atlantic (SCAR -A) regional experiment to support atmospheric correction. Having seen the need of atmospheric correction, Hadjimitist et al. (2004) mentioned related methods that can be used to solve the stated correction these are image-based method, atmospheric modelling and ground data during the satellite overpass.

However, Fallah et al. (1995) was interested and became inquisitive to know about the state of atmospheric corrected image. In their findings, they concluded that atmospheric corrected image has shown significant improvement in the classification of object-based analysis. Attention have been drawn by several scholars that in the study of earth surface or vegetal cover, there is greater need to unfolds surface contribution from the combined atmospheric reflectance and failure to do this will lead to sources of errors in the use of time series data for surface parameterization with satellites (Deschamps et al., 1983; Gordon et al., 1988; Justice et al., 1991; Tanr et al., 1992). This study seeks to address atmospheric correction on Landsat imagery using Remote sensing technique.

1.1 Objective of the Study

The objectives of the study were;

1. Discuss the types of atmospheric correction
2. Determine the Normalized Difference Vegetation Index using atmospheric corrected image
3. Highlight the Normalized Difference Vegetation Index without atmospheric corrected image

2.0 LITERATURE REVIEW

2.1 Types of Atmospheric Correction Theories

2.1.1 Dark Object Subtraction Model

The Dark Object Subtraction Model (DOSP) is an atmospheric correction method, also known as the histogram minimum method. The effect of haze is usually a relatively uniform elevation in spectral values in the visible bands of energy. One means of reducing haze in imagery is to look for values in areas of known zero reflectance, like deep water. Any value above zero in

GPR Journals
www.gprjournals.org
Journal of Environmental and Geographical Studies
ISSN 2958 - 4116 (Online)
Vol.2, Issue 1, pp 1 – 24, 2023

these areas is likely to represent an overall increase in values across the image and can be subtracted from all values. DSOP is regarded as the simplest atmospheric corrective measures which yield cloud free skies. Its principles stated that most of the dark objects are contributed by the atmosphere through the visible wavelength. Dark Object Subtraction model added benefit that it compensates for variations in solar output according to the time of year and the solar elevation angle. To do this, it requires the same estimate of the Dn of haze (e.g., the Dn of deep clear lakes), the date and time of the image, the central wavelength of the image band, the sun elevation, and radiance conversion parameters (Hadjimitsis et al., 2004a; Song et al.; 2001, Chavez, 1996).

2.1.2 Cost Model

The Cost model is known as cosine estimation of atmospheric transmittance and was developed by Chavez (1996) as a technique for approximation. Justification of cost model was reasonable by relative mean comparison of cosine estimation of $T\lambda^{\Theta}$ across Θ with $T\lambda^{\Theta}$ derived from atmospheric optical thickness and average across Θ and λ. It incorporates all of the elements of the Dark Object Subtraction model (for haze removal) plus a procedure for estimating the effects of absorption by atmospheric gases and Rayleigh scattering. It requires no additional parameters over the Dark Object Subtraction model and estimates these additional elements based on the cosine of the solar zenith angle (90 – solar elevation).

2.1.3 Full Correction Model

The full model is the most demanding in terms of data requirements. The model combines the parameters for the Dark Object Subtraction and Cost models which corrective input requires an estimate of the optical thickness of the atmosphere and the spectral diffuse sky irradiance (the down welling diffuse sky irradiance at the wavelength in question arising from scattering (Forster,1984; Turner and Spencer, 1972).

2.1.4 Apparent Reflectance Model

Apparent Reflectance Model is rarely used since it offers very little accommodation to atmospheric effect, it embraces the sun elevation and the effective thickness of the atmosphere. This method serves as a means of converting digital number into approximate reflectance values. Thekaekara et al., (1969) calculated spectral solar irradiance where they based their study on wavelength specification and it was interpolated from the look up table for annual variation, Julian days starts at noon – need to specify the hour in GMT (Cracknell & Hayes, 1991).

Optical thickness is the negative natural logarithm of the proportional transmittance of the atmosphere. Thus, a perfectly transparent atmosphere, with a transmittance of 1.00 has an optical thickness of 0.00. Optical thickness varies as primarily a function of Rayleigh scattering, aerosols, moisture and ozone content. Total optical thickness can be reasonably estimated as the sum of these major elements. Forster (1984) provides perhaps the best guidance on estimating these values. However, briefly, optical thickness due to Rayleigh scattering ranges from about 0.22 in the blue wavelengths, to 0.09 in the green, 0.05 in the red and 0.01 in the near-infrared. These values apply to a standard pressure of 1013 mbar at sea level. To adjust for standard pressure at a higher altitude, multiply the optical thickness by the ratio of the pressure at the new altitude by that at sea level. Aerosols are the primary determinants of haze.

GPR Journals
www.gprjournals.org
Journal of Environmental and Geographical Studies
ISSN 2958 - 4116 (Online)
Vol.2, Issue 1, pp 1 – 24, 2023

3.0 METHODOLOGY

Landsat image was downloaded from Global Land Cover Facility for 2003 and spatial resolution of 28.5 metres. The imagery was converted to radiance in Idrisi software and later converted the radiance map to temperature.

3.1 Radiance/Atmospheric Correction

Radiance converts raw satellite digital number values to calibrated radiances using lookup tables of gain and offset setting for Lansat satellites 1-5 and user-defined values for Lmin/Lmax or Offset/Gain for other sensor systems which are contained in the header file of the image concerning the metadata, that is acquisition date and Sun elevation angle (Chander et al., 2009). Conversion to radiances is used to facilitate comparisons between images from different dates. Chander et al., (2003) and severally applied the formula method to convert the DN values to at- satellite values (Abrams, 1999; Mathew, 2015). The formula was applied to each band of Landsat ETM+/TM bands 1-5, 7:

L (ƛ) = Grescale x DN (ƛ) + Brescale (Radiance = Band-specific rescaling gain factor x DN + Band-specific rescaling bias factor) 3.1

-where Band-specific rescaling gain factor is found in the header records, per specific band

-where DN is the pixel value resident in the specific band

-where Band-specific rescaling bias factor is found in the header records, per specific band.

3.2 The Study Area

The study area is Obio- Akpor Local Government Area. It is one of the cities in the Niger Delta where economic activities are heavily concentrated in Port Harcourt metropolis. The Geography of the LGA covered about 260 km^2 and is located between latitudes 4° 45'N and 4° 60'N and longitudes 6° 50°E and 8° 00'E (Egwuogu *et al.*, 2016). National population Census (2006) in the Department of (National Bureau of Statistics, 2006) gave the total population size of Obio-Akpor LGA as 464,789. Obio-Akpor is bounded by Port Harcourt (local government area) to the south, Oyigbo to the east, Ikwerre to the north, and Emohua to the west. Its headquarters is at Rumuodomaya and the population of the city therefore increases on a daily basis due the present multi-national Companies. Activities of these industries result into release of different gases and particles into the atmosphere. These emitted gases and particles react and dissolve in saturated water which precipitates to affect the quality of life. The area is mainly characterized by the indigenous people of the Ikwerre which cut across the four kingdoms namely Evo, Apara, Akpor and Rumueme (Wokocha & Omenihu, 2015).

3.3 Climate and Other Conditions

Climate condition of the place is noted by hot monsoon which characterized heavy rainfall throughout the rainy season in River State. The study area has nine Months of rainy season and three Months of dry season. It has an average of 250mm and 330 days of rain fall (Ayo et al., 2017). Eludoyin (2010) further described the relief of the place as lowland with average elevation between 20 to 30 m above the mean sea level. Geology comprises basically of alluvial sedimentary basin and basement complex and thick mangrove forest, raffia palms and light rainforest are the major types of vegetation found within the locality. Ayolagha, (2010) evaluated the soil nature and confirmed sandy and loamy underlain by a layer impervious pan and is always leached due to the heavy rainfall experienced in this area which inherently causes seasonal flooding. The study area is well drained with both fresh and salt water. The salt water is caused by the intrusion of sea water inland, thereby making the water slightly salty.

Journal of Environmental and Geographical Studies
ISSN 2958 - 4116 (Online)
Vol.2, Issue 1, pp 1 – 24, 2023

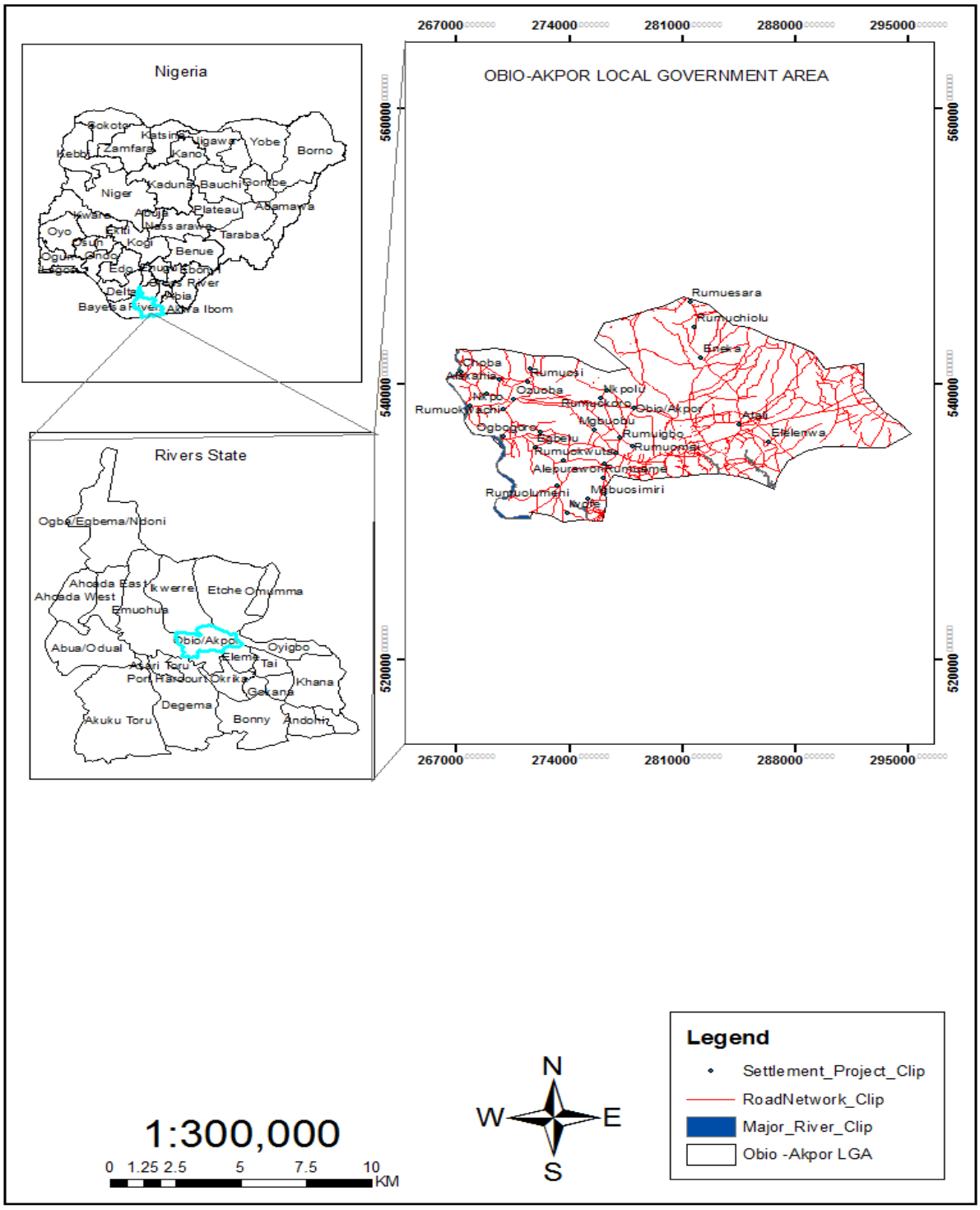

Figure 1: Map of the study area

Source: Authors (2022)

GPR Journals
www.gprjournals.org
Journal of Environmental and Geographical Studies
ISSN 2958 - 4116 (Online)
Vol.2, Issue 1, pp 1 – 24, 2023

4.0 RESULTS AND DISCUSSION

Conversion to top-of-atmospheric spectral radiance is a product of radiometrically corrected image pixels and that appropriate absolute radiometric calibration factor (also referred to as a K factor) to get band-integrated radiance [W-m-2-sr-1] and the result is through the division of the effective bandwidth (Keith, 2003) to get spectral radiance [W-m-2-sr-1-µm-1]. The Joint Agency Commercial Imagery Evaluation (JACIE) Team dated their ground truth measurement and confirmed Quick Bird absolute radiometric calibration factors (K factors) were recorded in the image metadata file (extension.IMD). They warned, for better image analytical results, conversions to band-integrated radiance or spectral radiance should be exercised using the factors listed in the technical note.

Radiance conversion involves two vital steps in the image operations. First, conversion of digital numbers in the thermal bands of Landsat TM/ETM (Bands 5, 6 and 7) to radiance and two to temperature values. Bands 2 and 3 were selected for radiance because of Normalized Difference Vegetation Index study. Figures 1 and 2 are good examples of radiance where user defined band specification was employed for the process, minimum and the maximum values of image were extracted. For band 3, spectral radiance at digital number (L mim) is 91.84 and spectral radiance at digital number (L max) is 256. Specially, band 4 spectral radiance at digital number (L mim) is 52.94 and the spectral at digital number (L max) is 256.

The second step is the conversion to temperature which procedure is quite different from radiance calculation. Here, the date of image capture, Month, year, Sun angle, influence of haze and time (GMT) is important in the atmospheric correction. Putting band 3 into consideration, image was captured by Global Land Cover Facility (GCLF) on the 22nd of December, 2003 at exactly 5.30 GMT. Digital number of hazes recorded by GLCF is 91.83984 and the sun angle or elevation at the point of image capture is sixty degrees [60°]. Spectral solar irradiance [EO] is 135.1 and satellite viewing angle is zero [0]. Maximum digital number for atmospheric corrected is 1023 while its upper limited value is 0.00 and lower limited value shows 0.88 as shown in figure 4.

Similarly, sun angle or elevation, spectral solar irradiance [E0] and the satellite viewing angle of band 4 is the same with that of band 3 as given above. The difference is that digital number of hazes in band 4 is 52.9375 and figure 5 showed atmospheric corrected for band 4 with upper limit of 0.00 and lower limit of 1.0 for the image processing. The study noted that dark object subtraction method extracted from the literature search proved to be the best among the corrective measures.

Journal of Environmental and Geographical Studies
ISSN 2958 - 4116 (Online)
Vol.2, Issue 1, pp 1 – 24, 2023

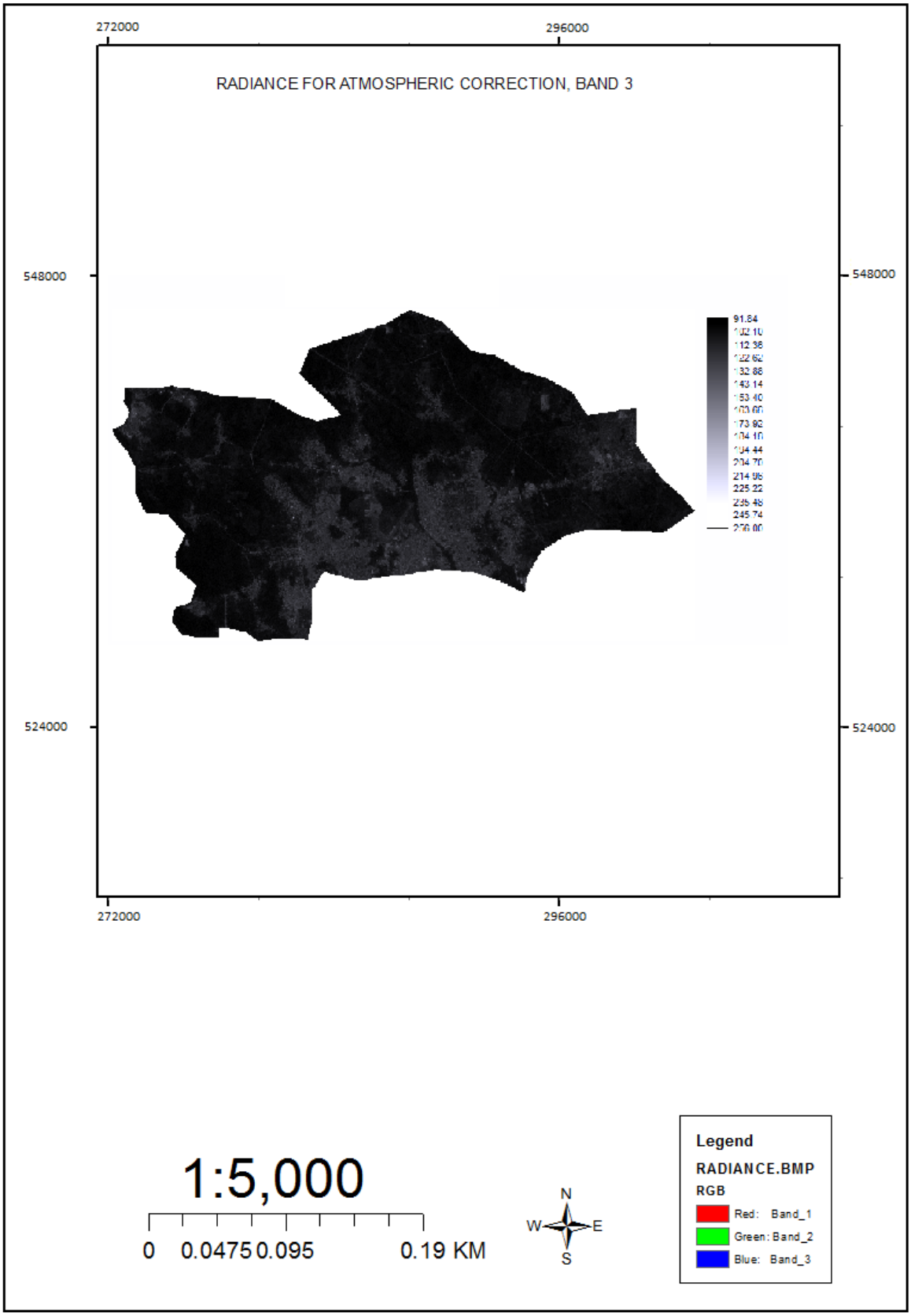

Figure 2: Radiance for atmospheric correction, Band 3

Journal of Environmental and Geographical Studies
ISSN 2958 - 4116 (Online)
Vol.2, Issue 1, pp 1 – 24, 2023

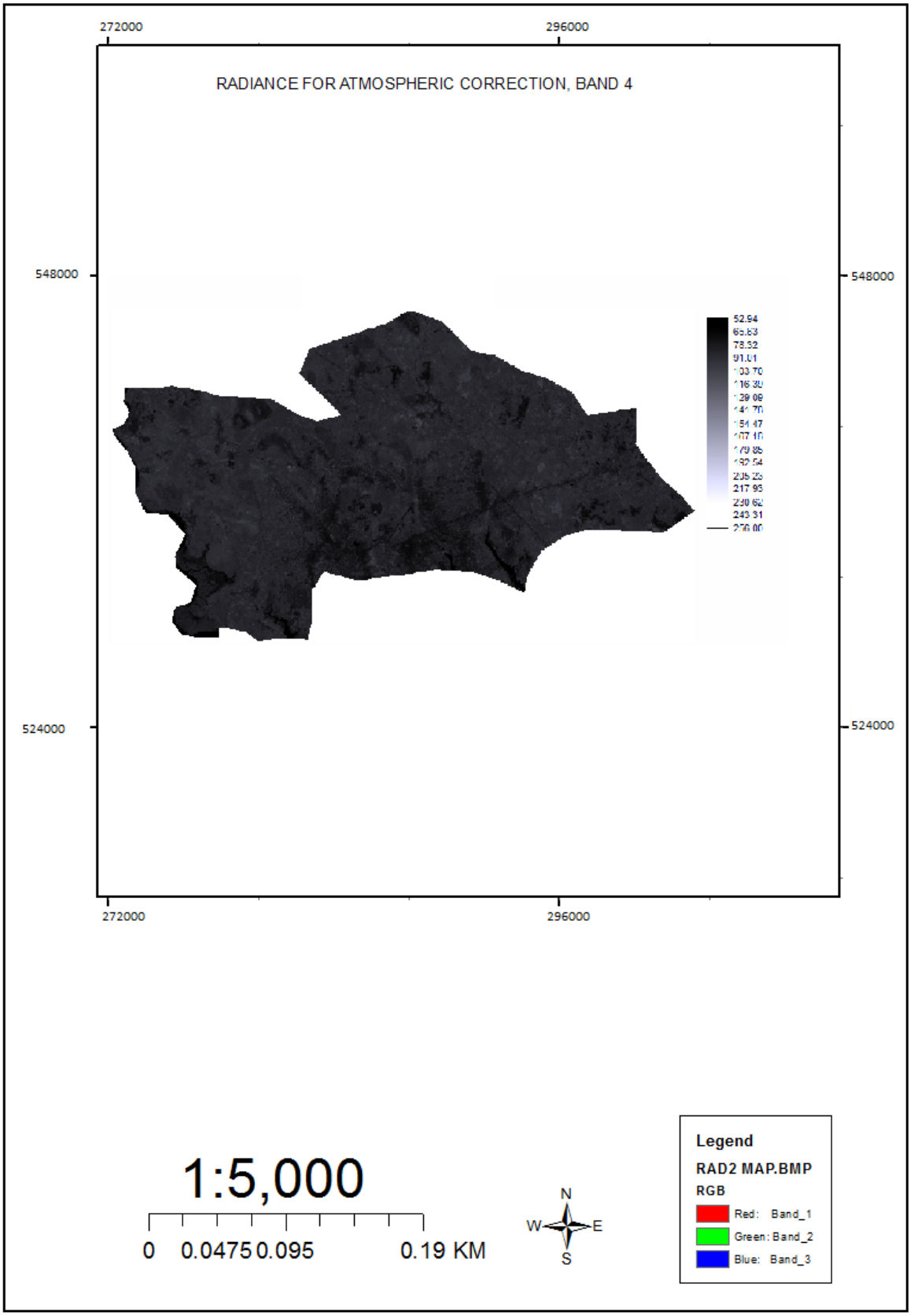

Figure 3: Radiance for atmospheric correction, Band 4

Journal of Environmental and Geographical Studies
ISSN 2958 - 4116 (Online)
Vol.2, Issue 1, pp 1 – 24, 2023

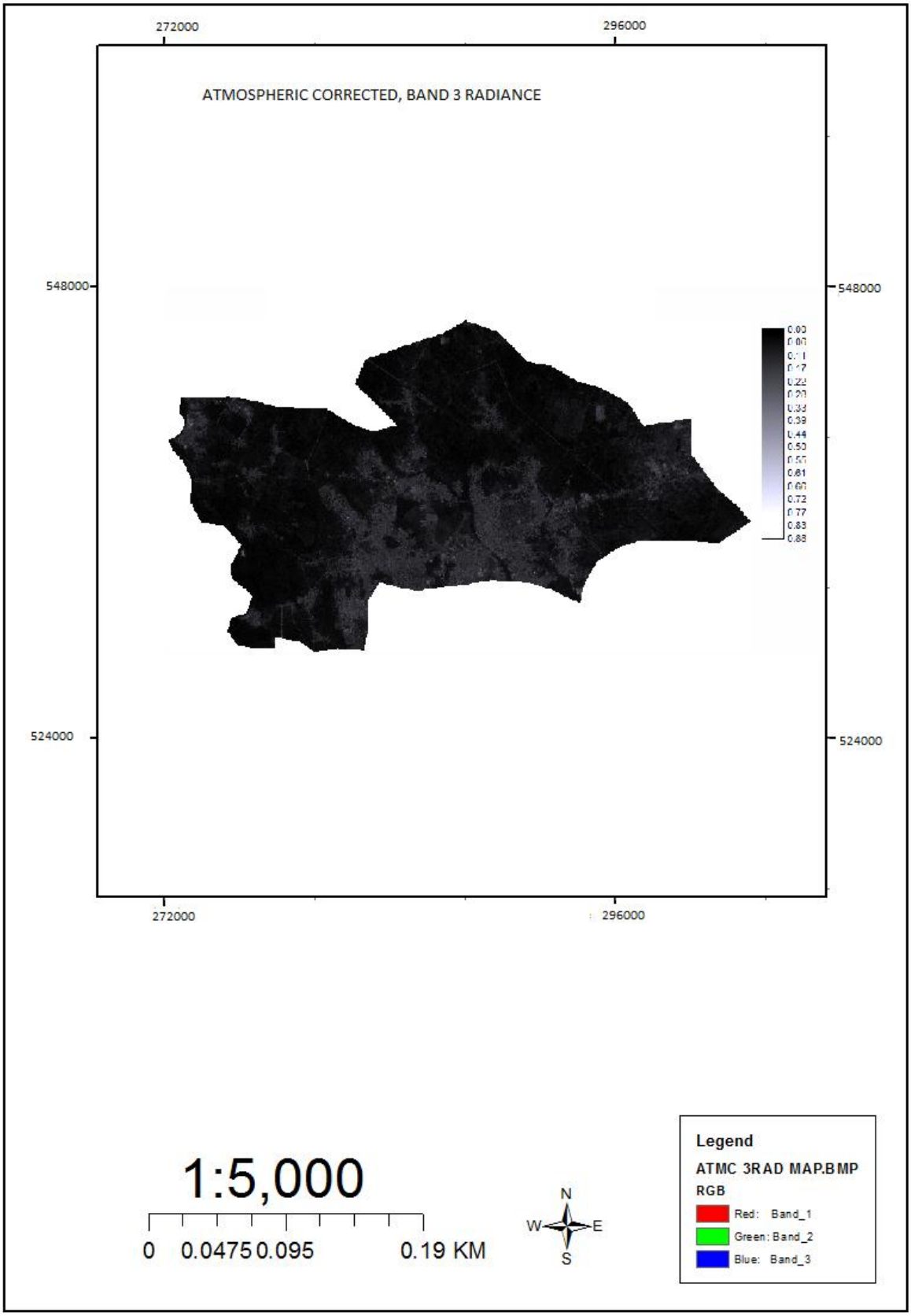

Figure 4: Atmospheric corrected, Band 3 radiance

Journal of Environmental and Geographical Studies
ISSN 2958 - 4116 (Online)
Vol.2, Issue 1, pp 1 – 24, 2023

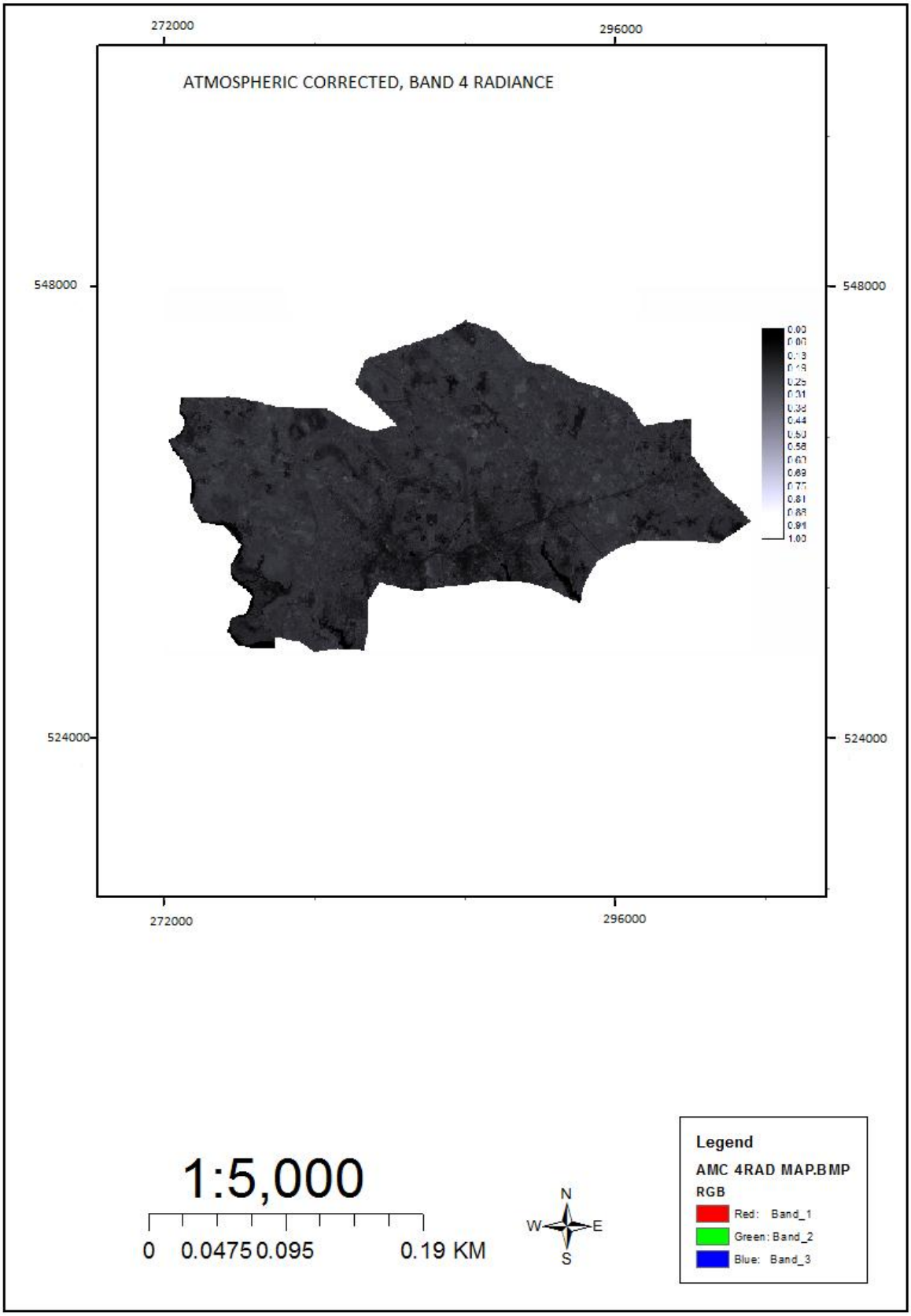

Figure 5: Atmospheric corrected, Band 4 radiance

GPR Journals
www.gprjournals.org
Journal of Environmental and Geographical Studies
ISSN 2958 - 4116 (Online)
Vol.2, Issue 1, pp 1 – 24, 2023

4.1 NORMALIZED DIFFRENCE VEGETATION INDEX (NDVI)

The Normalized Difference Vegetation Index (NDVI) was first predicted by Rouse et al. (1973) to measure the reflectance ratio of energy that is reflected from an object to the energy incident on the object (Kumar & Silva, 1973). Spectral reflectance data can be used to compute a variety of vegetative indices whether crops are well grown in their state of plantation as well as correlation with agronomic and biophysical plant parameters related to photosynthetic activity and plant productivity (Ma et al., 2001; Adamsen et al., 1999). Research Community however, defined it as a physical indicator that uses both visible and near-infrared bands of the electromagnetic spectrum, to analyse green vegetation canopy. Major application areas of NDVI are crop yields (Li et al., 2010; Casadesus et al., 2007), pasture performance, ground parameters such as percentage of ground cover ((Mullan and Reynolds, 2010), photosynthesis activity, surface water, leaf area index (Liu & Pattey, 2010) and the amount of biomass (Roderick et al., 1996).

Holme et al. (1987) examined vegetation status and vehemently stated that healthy vegetation will absorb most of the visible light that falls on it, and reflects a large portion of the near-infrared light while sparse vegetation reflects more visible light and less near-infrared light. Bare soils on the other hand reflect moderately in both the red and infrared portion of the electromagnetic spectrum.

The NDVI is calculated from reflectance measurements in the red and near infrared (NIR) portion of the spectrum:

NDVI= (NIR-RED) / (NIR+RED

Where NIR is the reflectance of NIR radiation and Red is the reflectance of visible red radiation.

Theoretically, NDVI values are represented as a ratio ranging in value from -1 to 1 but in practice extreme negative values represent water, values around zero represent bare soil and values over 6 represent dense green vegetation. Results of the NDVI without atmospheric correction (Figure 6) show six division on the vertical scale bar, these are black region (<61.00), pink (69.70), brown colour (76.53 to 113.52), white (122.27 to 151.32), the green part is moving across 139.77 to 183.50 while outside the boundary consideration (192.25 to 201.00). These spectral properties depict different land cover within Obio- Akpor Local Government Area of Rivers State. The results are very impressive in the sense that the black region marks the water body of the area. Pink in the classification described the vegetation belt and white colour is an indication of bare soil within the built-up area. Brown area is a combination of built up and little part of vegetation were as the green is not pronounced due to colour encoding.

Atmospheric corrected NDVI (Figure 7) ranges from 0.00 to 1.00 which conformed to the theory of NDVI. Surely, four classes are very visible on the classified image and these are black, pink, white and brown. Black and pink represent water body due to its shape and have specification range from 0.02 to 0.01 on the vertical scale bar. There are light and dark brown aspect of the image which assume built up and vegetation. Bare soil takes white colour in the colour coding and green is still hidden due to influence.

In furtherance of the study above, predicted NDVI was also analysed to evaluate the state of the vegetation. Both the atmospheric corrected and uncorrected where used to account for the greenish state of the Obio-Akpor Local Government Area. This study became inquisitive because the first and second analysis on vegetal class did not give rise to the true picture, green

Journal of Environmental and Geographical Studies
ISSN 2958 - 4116 (Online)
Vol.2, Issue 1, pp 1 – 24, 2023

vegetation. For vegetation (green) and water body (blue) to be in their natural state, atmospheric corrected NDVI was made constant while uncorrected NDVI became a dependent factor which undoubtedly resulted to predict NDVI as shown in figure 8.

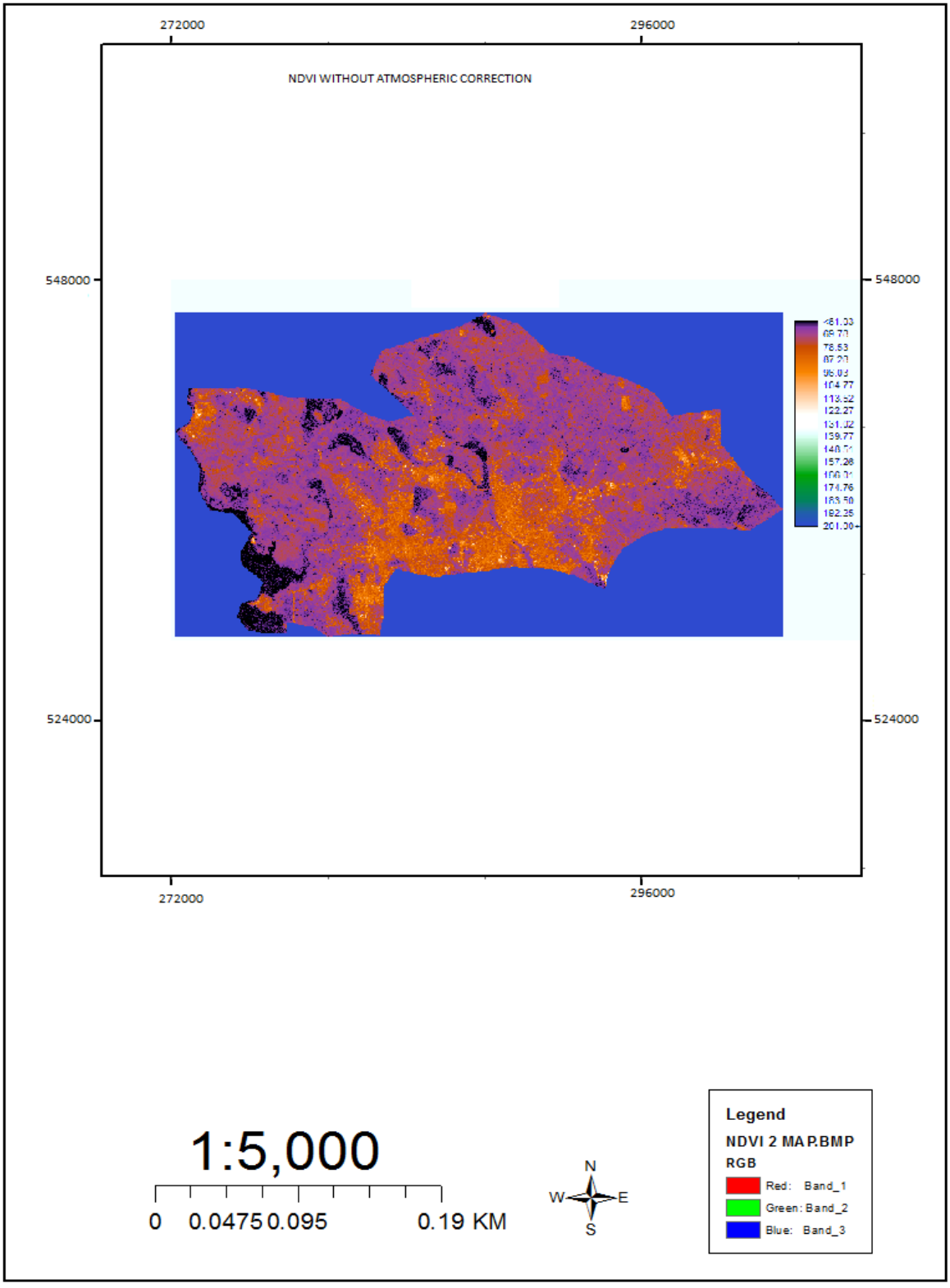

Figure 6: NDVI without atmospheric correction

Journal of Environmental and Geographical Studies
ISSN 2958 - 4116 (Online)
Vol.2, Issue 1, pp 1 – 24, 2023

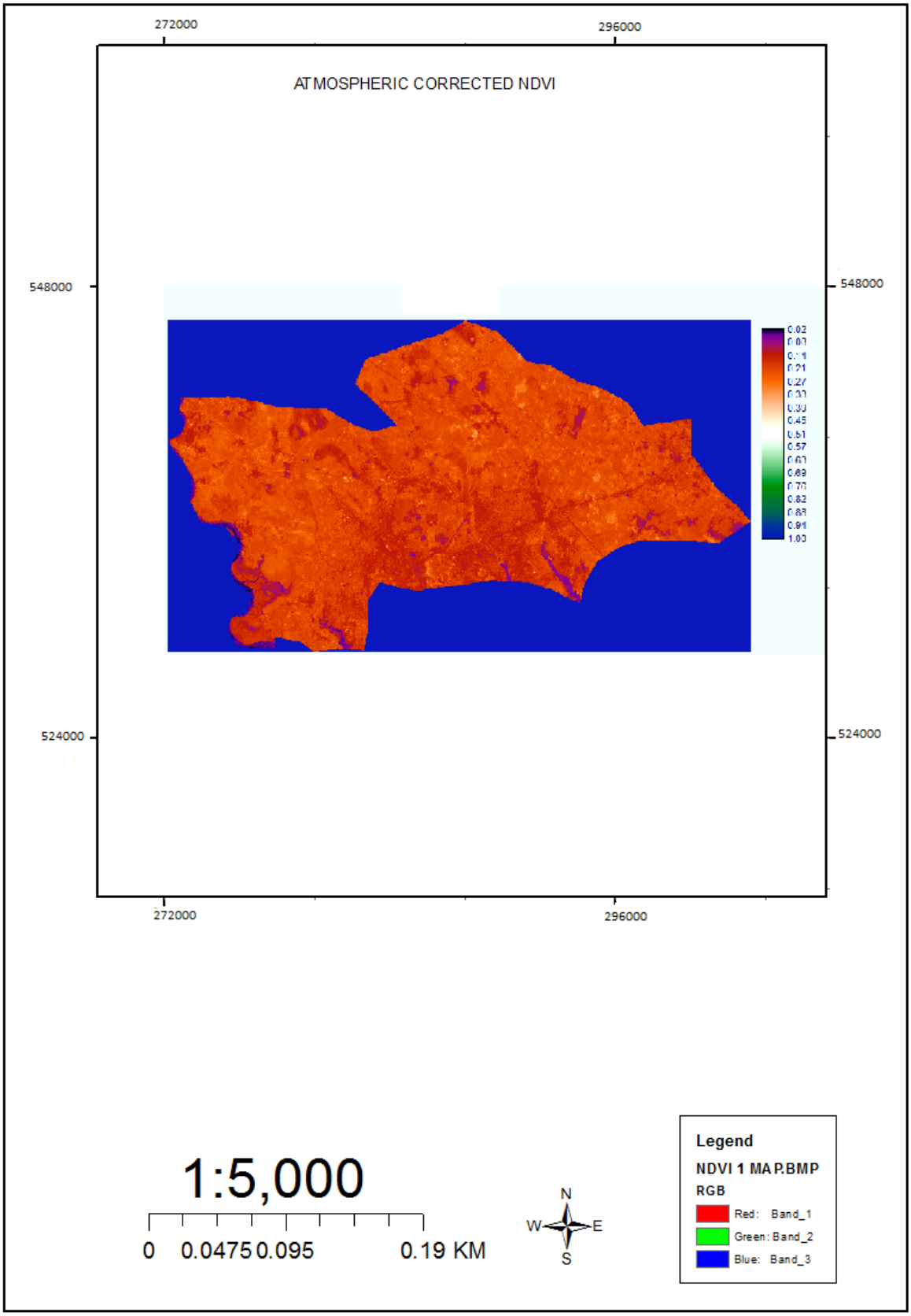

Figure 7: NDVI with atmospheric correction

Journal of Environmental and Geographical Studies
ISSN 2958 - 4116 (Online)
Vol.2, Issue 1, pp 1 – 24, 2023

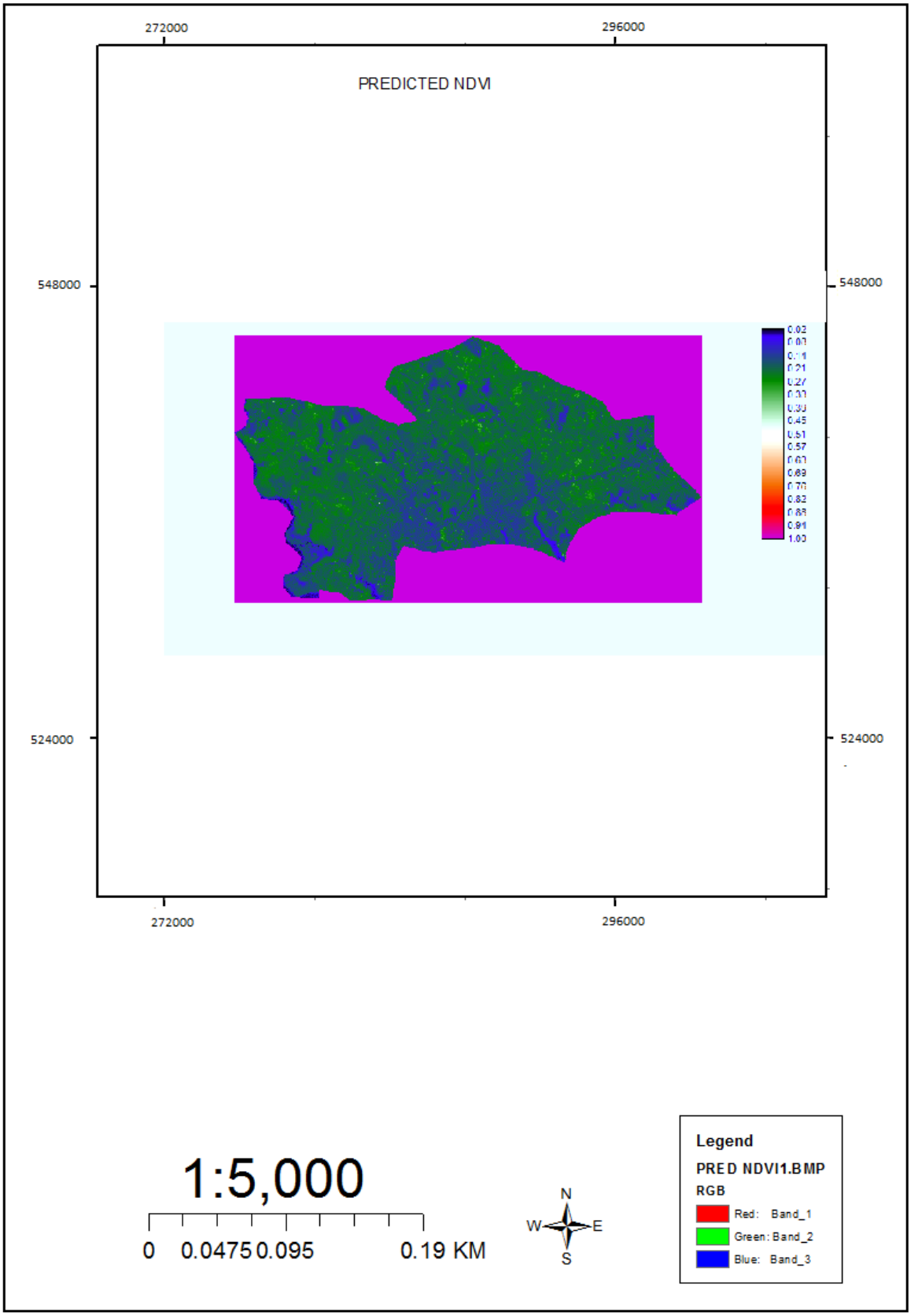

Figure 8: Predicted NDVI

GPR Journals
www.gprjournals.org
Journal of Environmental and Geographical Studies
ISSN 2958 - 4116 (Online)
Vol.2, Issue 1, pp 1 – 24, 2023

4.2 REGRESSION ANALYSIS

Regression undertakes either linear or multiple to analyse the relationship of one or more independent variables to a single dependent variable (Kleinbaum et al., 1988; Clark & Hosking, 1986). Both methods were widely used to justify Normalized Difference Vegetation Index in terms of atmospheric corrected and uncorrected images to see the behaviour of the canopy state whether they are stressed or not. Linear regression developed nine parameters which were used to define NDVI relationship between atmospheric corrected and uncorrected spatially. The parameters are coefficient of determination (99.15), standard deviation of X (91.513), standard deviation of Y (0.399211), sum of errors of estimate (0.036718), sample size of 583347 and the degree of freedom is 583345. A model was created at the end of the analysis which proved high correlation with a mean value of 0.004344 and constant of -0.113712. Finally, both linear and multiple regression conform to rules of NDVI (Figures 5.8 and 5.9), while Table 1 is the statistics for the regression that show the adjusted R and adjusted R square of one (1).

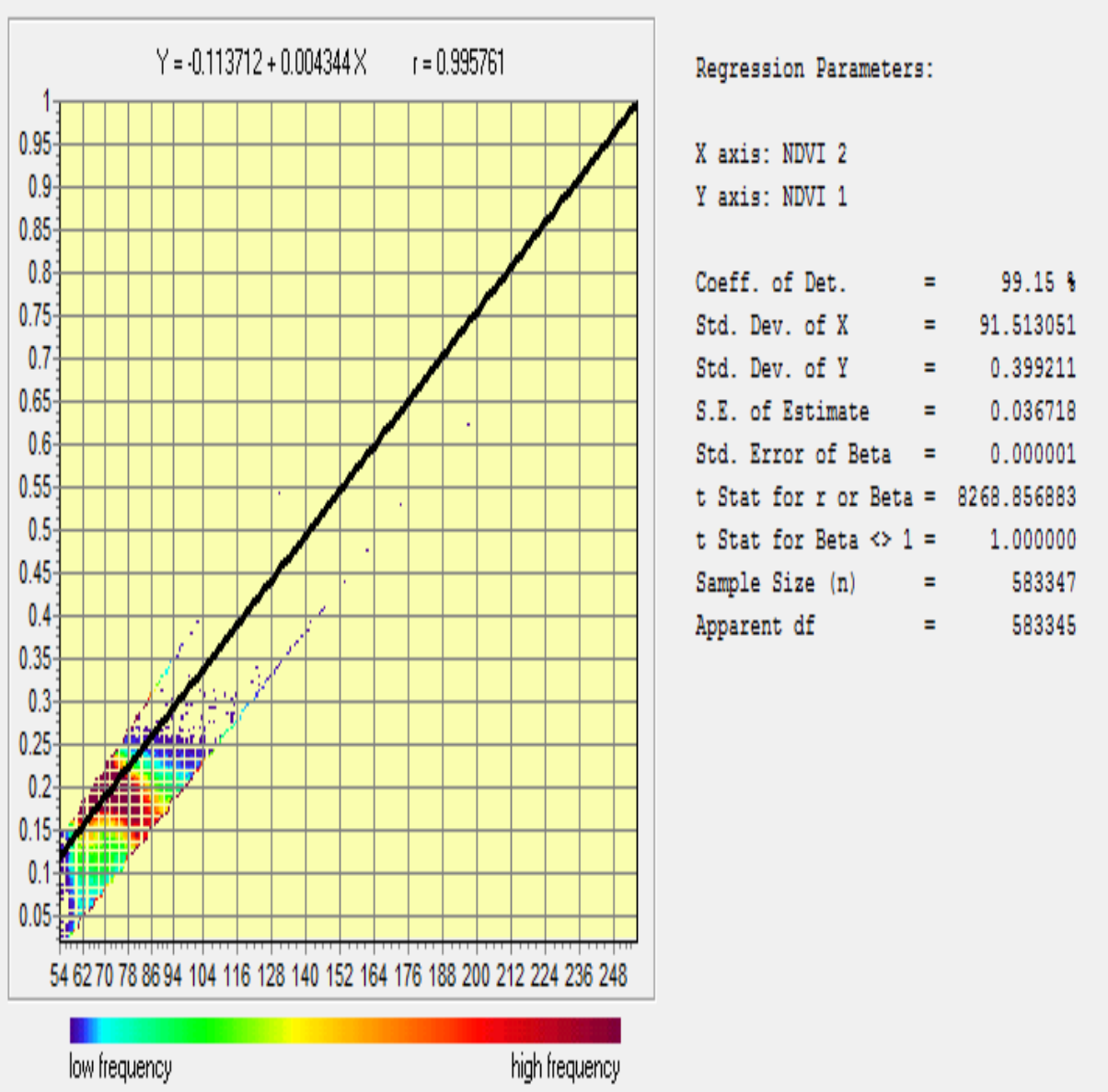

Figure 9: Regression model for NDVI

GPR Journals
www.gprjournals.org
Journal of Environmental and Geographical Studies
ISSN 2958 - 4116 (Online)
Vol.2, Issue 1, pp 1 – 24, 2023

Regression equation:

NDVI 1 = -0.0000 + 1.0000*NDVI 1 + 0.0000*NDVI 2

Regression statistics:

Apparent R = 1.000000 Apparent R square = 1.000000

Adjusted R = 1.000000 Adjusted R square = 1.000000

F (2,583344) = 46483.773438

Table 1: ANOVA regression results

Source	Apparent degrees of freedom	Sum of squares	Mean square
Regression	2	92967.55	46483.77
Residual	583344	0.00	1.00
Total	**583346**	**92967.55**	

Table 2: Individual regression coefficients

Source	Coefficient	t_test (583344)
Intercept	-0.000000	-0.000000
NDVI 1	1.000000	28.043886
NDVI 2	0.000000	0.000000
Total	**583346**	**92967.55**

Journal of Environmental and Geographical Studies
ISSN 2958 - 4116 (Online)
Vol.2, Issue 1, pp 1 – 24, 2023

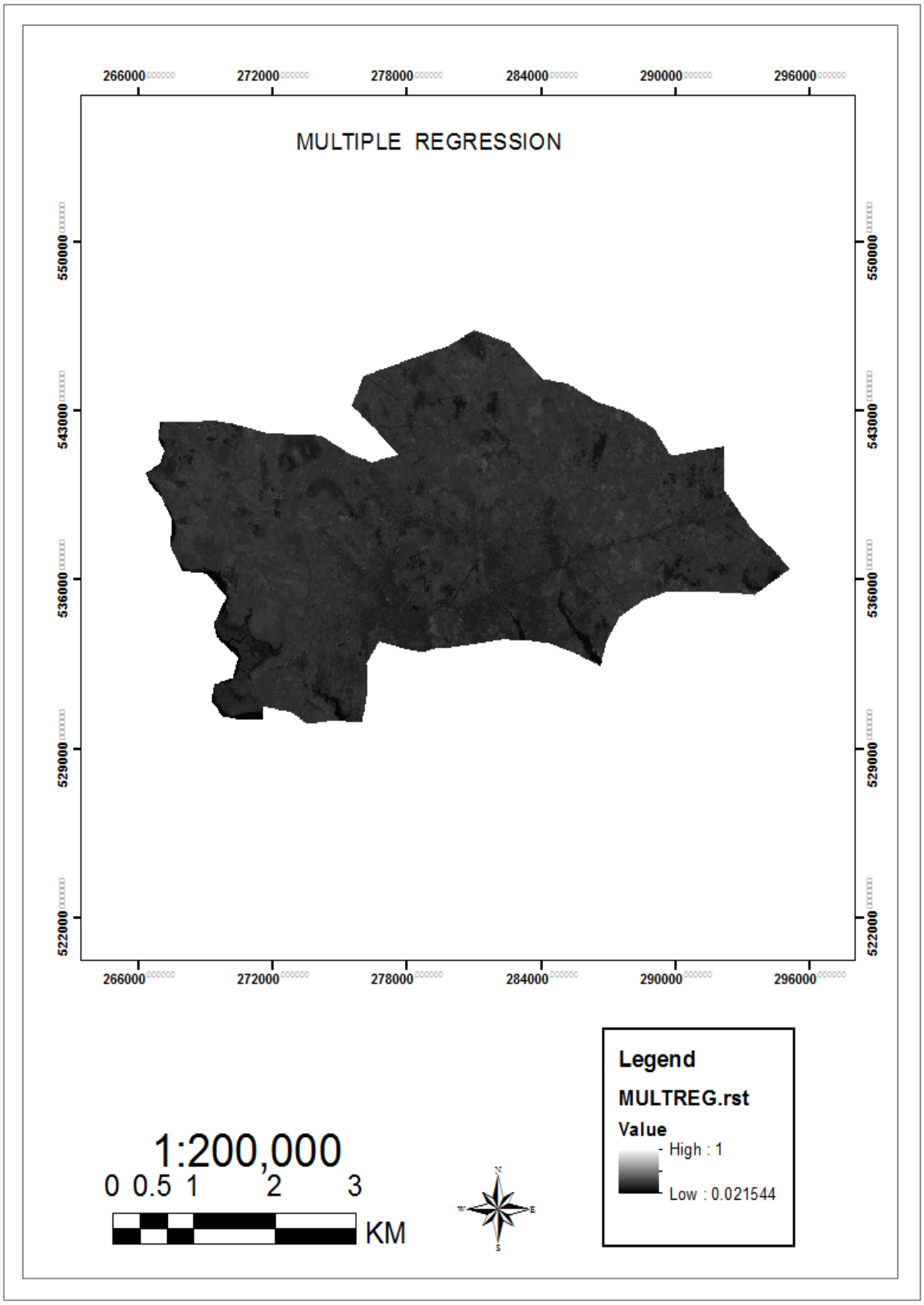

Figure 10: Multiple regression of normalized difference vegetation index

GPR Journals
www.gprjournals.org
Journal of Environmental and Geographical Studies
ISSN 2958 - 4116 (Online)
Vol.2, Issue 1, pp 1 – 24, 2023

4.3 SOIL ADJUSTED VEGETATION INDEX (SAVI)

The soil adjusted vegetation index is a distance-based operation to actuate for vegetation indices and to compensate for the effects of disturbing factors on the relationships between vegetation spectral reflectance as measured by crop characteristics, such as crop type, leaf area index (LAI), or canopy biomass. SAVI is one of the vegetation indices used to account for soil background and atmospheric conditions to annul the effect of soil brightness where vegetation is sparse. SAVI tends to minimize soil brightness, a phenomenon that has been demonstrated by many researchers. Huete et al., (1988) nevertheless, in a view to optimize crop performance introduced a soil calibration factor in the NDVI equation to account for the first order soil-vegetation optical interactions which serves as a bases for study and discussion in the field of academia. SAVI is a compromise between NDVI and perpendicular vegetation index (PVI) and is defined as ;

$$SAVI = (Pir - Pr) / (Pir + Pr + L) \times (1+L)$$

Where L is a constant that is a surrogate for LAI. Huete *et al.* (1988) and Chehbouni *et al.*, (1994) defined the optimal adjustment factor of L = 0.25 to be considered for higher vegetation density in the field, L = 0.5 for intermediate vegetation density, and L = 1 for the low vegetation density. He suggested that SAVI (L = 0.5) successfully minimized the effect of soil variations in green vegetation compared to NDVI. Casanova et al., (1998) further envisage that PVI is a correct standard for soil reflectance in linear and less-scattered relationship with the fraction of intercepted photo- synthetically active radiation (fPAR) than NDVI.

Figure 10 is soil adjusted vegetation index map. It is another way to compensate for canopy variability among crops in a given area under consideration. Huete et al., (1988) and Chehbouni et al., (1994) factors were recalled to dynamic research. L equals to one was invoked to algorithms because of low vegetation density. The result illuminated negative value (-0.47) at the upper scale and at the lower is 0.22. Vegetation occupies (-0.34 to -0.17), blue covered water on the vegetation (-0.43 to -0.34) which is suspected to be rain droplet or dew. Water body appears red in colour from negative to positive value (-0.00 to 0.18). Bare soil has (-0.17 to 0.13) which is interlinked with built up. Critically, there is loss in vegetation as a result of human impact and loss of rain water. Water body has lower reflection, it reflects electromagnetic energy in the visible up to the near infrared. Beyond 1.2 µm all energy is absorbed and this led to increase in mass while surface reflectance from bare soil is dependent on so many factors and the influential factors are soil colour, moisture content, the presence of carbonates and iron oxide content. The result revealed a proportional gained in bare land (soil).

Journal of Environmental and Geographical Studies
ISSN 2958 - 4116 (Online)
Vol.2, Issue 1, pp 1 – 24, 2023

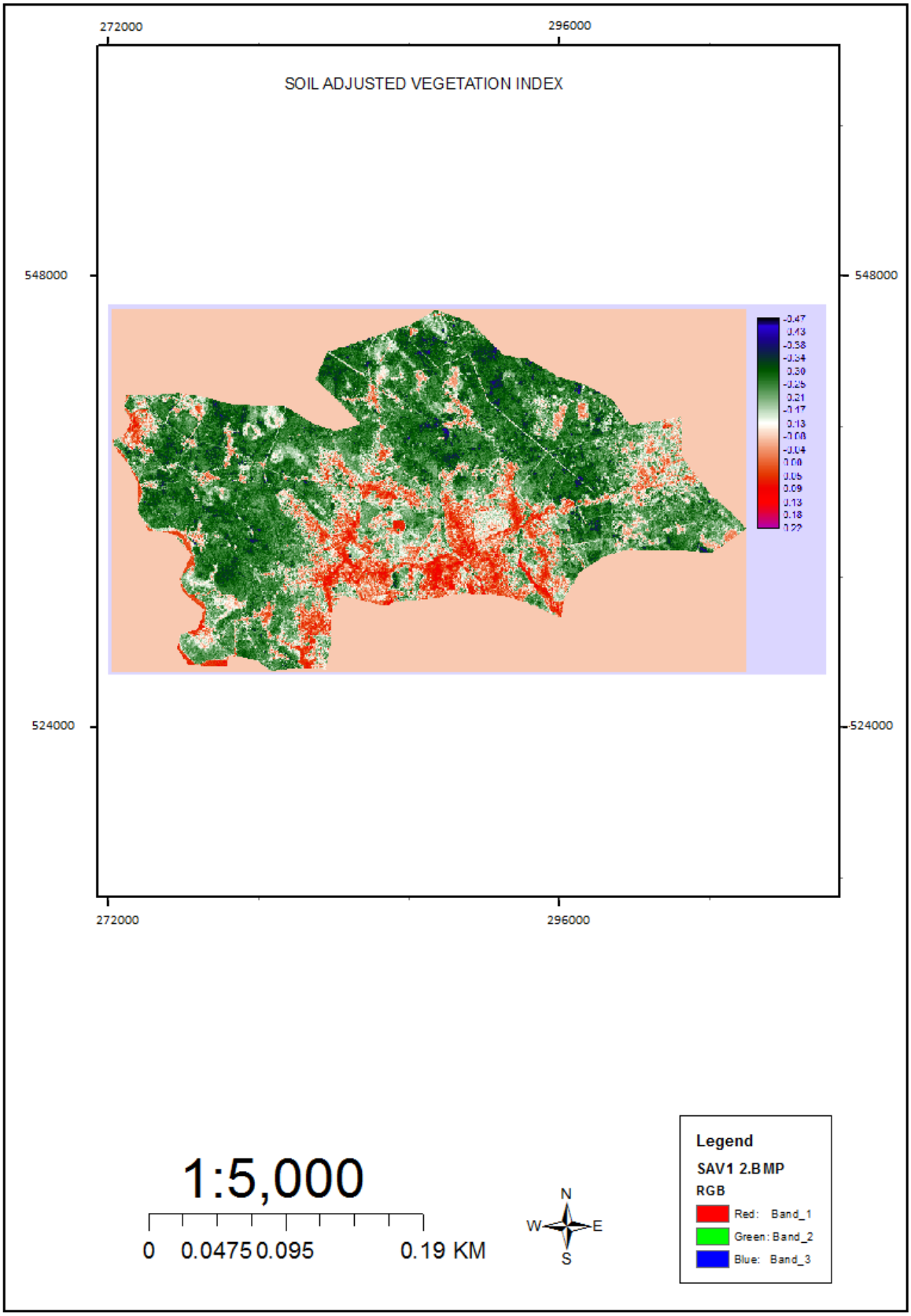

Figure 11: Soil adjusted vegetation index

Journal of Environmental and Geographical Studies
ISSN 2958 - 4116 (Online)
Vol.2, Issue 1, pp 1 – 24, 2023

5.0 CONCLUSION

The study assessed the different atmospheric correction methods and dark object subtraction techniques was vigorously used for the analysis. Atmospheric corrected and uncorrected Landsat 2000 TM images were used to analysed Normalized Different Vegetation Index (NDVI) and Soil Adjusted Vegetation Index (SAVI). Analysis showed that atmospheric corrected image gives a good reflectance result than uncorrected image. Atmospheric corrected NDVI started from 0.02 to 1.0 on the scale of measurement while uncorrected NDVI ranges from <61.00 to 201. SAVI results intensified the NDVI which scientifically confirmed the range of -0.47 to 0.22 and a linear model was produced to back the research study. Vegetation Indices highlighted the amount of vegetation, the difference between vegetation and soil is so glaring, and atmospheric effects should be reduced.

6.0 RECOMMENDATION

Having seen the results of the study, it is recommended that for image studies to be carried out, there should be an atmospheric correction to have a precise result.

REFERENCES

Abrams, M., Hook, S., & Ramachandran, B. (1999). ASTER User Handbook, Version 2, NASA/Jet Propulsion Laboratory, Pasadena.

Adamsen, F.J., Pinter, P., Barnes, E., LaMorte, R., Wall, G., Leavitt, S., & Kimball, B. (1999). Measuring wheat senescence with a digital camera. Crop Sci 39: 719–724.

Ayolagha, G. (2010). Department of soil Sci, Rivers State University of Science and Technology, Research Journal of Environmental and Earth Sciences 3 (4): 307-313, 2011.

Ayo-Enwerem, C.M., Ahaotu, E.O., Nwogu, C.M., & Esukpa, M. (2017). Haematology and Serum Biochemistry of Starter Broiler fed Diets Contaminated Red Sandalwood (Pterocarpus Santoliniodes) Leaf Meal. Direct Research Journal of Veterinary Medicine and Animal Science. 2(4), 111-114.

Berk, A., Bernstein, L.W., & Robertson, D.C. (1989). MODTRAN: A moderate resolution model for LOWTRAN 7. GL-TR-89-0122, AFGL, Hanscomb AFB, MA, USA.

Casadesus, J., Kaya, Y., Bort, J., Nachit, M.M., Araus, J.L., Amor, S., Ferrazzano, G., Maalouf, F., Maccaferri, M., & Martos, M. et al. (2007). Using vegetation indices derived from conventional digital cameras as selection criteria for wheat breeding in water-limited environments. Ann App Bot 150: 227–236.

Casanova, D., Epema, G.F., & Goudriaan, J. (1998). Monitoring rice reflectance at field level for estimating biomass and LAI. *Field Crop Res. 55*, 83–92

Chander, G. & Markham, B.L. (2003). Revised Landsat-5 TM radiometric Calibration Procedures, and Post calibration Dynamic Ranges. IEEE Transactions on Geoscience and Remote Sensing, 41, 2674–2677.

Chander, G., Markham, B.L., & Helder, D.L. (2009). Summary of Current Radiometric Calibration Coefficients for Landsat MSS, TM, ETM+, and EO-1 ALI Sensors. Remote Sensing of Environment 113 (2009) 893–903.

Chavez, P. S. (1996). Image-Based Atmospheric Corrections – Revisited and Improved, Photogrammetric Engineering and Remote Sensing, 62, 9, 1025-1036.

Journal of Environmental and Geographical Studies
ISSN 2958 - 4116 (Online)
Vol.2, Issue 1, pp 1 – 24, 2023

Chehbouni, J. Qi. A., Huete, A.R., Kerr, Y.H., & Sorooshian, S. (1994). A Modified Soil Adjusted Vegetation Index. Remote Sens. Environ. 48:119-126.

Chrysoulakis, N., Abrams, M., Feidas, H., & Arai, K. (2010). Comparison of atmospheric correction methods using aster data for the area of Crete: the ATMOSAT project, Int. J. Remote Sens.

Clark, W. A. V. & Hosking, P.L. (1986). Statistical Methods for Geographers. New York: John Wiley & Sons.

Cracknell, A. P., & Hayes, L. W. B. (1991). Introduction to Remote Sensing, (London: Taylor and Francis). Department of Crop and Soil Science, University of Port Harcourt, P.M.B 2353 Port Harcourt, Nigeria. Journal of Environment and Earth Science. www.iiste.org ISSN 2224-3216 (Paper) ISSN 2225-0948 (Online) Vol.5, No.13

Deschamps, P.Y., Herman, M., & Tanre, D. (1983). Modeling of the atmospheric effects and its application to the remote sensing of ocean colour. Applied Optics, 22, 3751- 3758.

Eludoyin. O. S. (2010). Department of Geography and Environmental Management. University of Port Harcourt, Port Harcourt. Research Journal of Environment and Earth Sc. 3(4): 307-313, 2011.

Fallah-Adl, J. J'aJ'a, S. Liang, Y. J. Kaufman & Townshend, J. (1995). Efficient Algorithms for Atmospheric Correction of Remotely Sensed Data, to appear in Proceedings Supercomputer '95, IEEE Computer Society Press.

Forster, B. C., (1984). Derivation of atmospheric correction procedures for LANDSAT MSS with particular reference to urban data. *International Journal of Remote Sensing*, 5, 5, 799-817.

Gordon, H.R., Brown, J.W., & Evans, R.H. (1988). Exact Rayleigh scaterring calculations for use with the Nimbus-7 Coastal Zone Color Scanner. Applied Optics,27,862-871

Hadjimitsis, D. G., Clayton, C. R. I., & Hope, V. S. (2004a). An assessment of the effectiveness of atmospheric correction algorithms through the remote sensing of some reservoirs, Int. J. Remote Sens., 25, 3651–3674.

Hadjimitsis, D. G., Clayton, C. R. I., & Hope, V. S. (2004a). An assessment of the effectiveness of atmospheric correction algorithms through the remote sensing of some reservoirs, Int. J. Remote Sens., 25, 3651–3674.

Holben, B. N., Eck, T. F., Slutsker, I., Tanr, D., Buis, J. P., Setzer, A., Vermote, E. F., Reagan, J. A., Kaufman, Y. J., Nakajima, T., Lavenu, F., Jankowiak, I., & Smirnov, A. (1998). AERONET - A federated instrument network and data archive for aerosol characterization. Remote Sensing of Environment, 66(1), 1-16.

Holben, B.N., Vermote, E., Kaufman, Y.J Tanr, D & Kalb, V. (1992). Aerosol Retrieval over Land from AVHRR data-Application for Atmospheric Correction. IEEE Trans. on Geosci. and Rem. Sens.,30,212-222

Holme, A. MCR., Burnside, D.G. & Mitchell, A.A. (1987). The development of a system for monitoring trend in range condition in the arid shrublands of Western Australia. Australian Rangeland Journal 9:14-20.

Journal of Environmental and Geographical Studies
ISSN 2958 - 4116 (Online)
Vol.2, Issue 1, pp 1 – 24, 2023

Huete, A.R., & Jackson, R.D. (1988). Soil and atmosphere influences on the spectra of partial canopies. *Remote Sens. Environ. 25*, 89–105

International Institute for Geo-Information Science and Earth Observation. (2004). Principle of Remote Sensing, Hengelosestraat 99, P.O. Box 6,7500 AA Enschede, Netherlands.

Justice, C.O., Eck, T.F., Tanr, D & Holben, B.N. (1991). The effect of water vapour on the normalized difference vegetation index derived for the Sahelian region from NOAA AVHRR data. Int. J. Remote Sensing, 12, 1165-1187

Kaufman, Y. J., Tanre, D., Remer, L., Vermote, E., A. Chu and Holben, B. (1997). Operational Remote Sensing of tropospheric aerosol over land from EOS moderate resolution imaging spectroradiometer, J. Geoph. Res. Vol. 102, No14, pp17051-17067

Keith, k. (2003). Radiance Conversion of Quick Bird Data. Technical Note

Kleinbaum, D. G., Kupper, L.L & Muller, K.E. (1988). Applied Regression Analysis and Other Multivariable Methods. Boston: PWS-KENT Publishing Company.

Kneizys, F. X., Shettle, E. P., Abreu, L. W., Anderson, G. P., Chetwynd, J. H., Gallery, W. 0., Selby, J. E. A. & Clough, S. A. (1988). Users guide to LOWTRAN 7. Air Force Geophysics Laboratory Hans comb AFB, Massachusetts. AFGL-TR-88-0177.

Kumar, R.., & Silva, L. (1973). Light Ray tracing through a leaf cross-section. Appl. Optics 12, 2950–2954.

Li, Y., Chen, D., Walker, C.N., & Angus, J.F. (2010). Estimating the nitrogen status of crops using a digital camera. Field Crop Res 118: 221–227.

Liu, J.G., &Pattey, E. (2010). Retrieval of leaf area index from top-ofcanopy digital photography over agricultural crops. Agr Forest Meteorol 150: 1482–1490.

Ma, B.L., Morrison, M.J., & Dwyer, L.M. (1996). Canopy light reflectance and field greenness to assess nitrogen fertilization and yield of corn. Agronomy J. 88:915-920.

Mathew, M. G. (2015). Converting Advanced Himawari Imager (AHI) Radiance Units Cooperative Institute for Meteorological Satellite Studies (CIMSS) University of Wisconsin-Madison E-mail: matg@ssec.wisc.edu

Mullan, D., & Reynolds, M. (2010). Quantifying effects of ground cover on soil water evaporation using digital imaging. Funct Plant Biol 37: 703–712.

Roderick, M., Smith, R.C.G., & Ludwick, G. (1996). Calibrating long term AVHRR- derived NDVI imagery. Remote Sensing of Environment 58: 1-12.

Roger, J.C., Eric, V & Nazi, E. S. (1994). Atmospheric Correction of MAS data during SCAR-An experiment. Atmospheric Sensing and Modeling, Rome, Italy, September 29-30, SPIE proceedings, Vol 2311, pp 83-89.

Rouse, J. W., Haas, R.H., Schell, J.A., & Deering, D.W. (1973). Monitoring vegetation systems in the Great Plains with ERTS, Third ERTS Symposium, NASA SP-351 I, 309- 323.

Running, S.W., Justice, C., Salomonson, V., Hall, D., Barker, J., Kaufman, Y., Strahler, A., Huete, A., Muller, J.P., Vanderbilt, V., Wan, Z.M., Teillet, P., & Carneggie, D. (1994). Terrestrial remote sensing science and algorithms planned for EOS/MODIS.

Journal of Environmental and Geographical Studies
ISSN 2958 - 4116 (Online)
Vol.2, Issue 1, pp 1 – 24, 2023

Song, C., Woodcock, C.E., Seto, K.C., Lenney, M.P., & Macomber, S.A. (2001). Classification and change detection using Landsat TM data: when and how to correct atmospheric effects? Remote Sensing of Environment, 75, 230-244.

Tanré, D., Deroo, C., Duhaut, P., Herman, M., Morcrette, J.J., Perbos, J. & Deschamps, P.Y. (1990). Description of a computer code to simulate the satellite signal in the solar spectrum: the 5S code. International Journal of Remote Sensing, 11 (4), 659-668.

Tanré, D., Holben, B.N., & Kaufman, Y.J. (1992). Atmospheric correction algorithm for NOAA-AVHRR products: theory and application. IEEE Transactions on Geoscience and Remote Sensing, 30 (2), 231-248.

Thekaekara, M. P., Kruger, R., & Duncan, C.H. (1969). Solar Irradiance Measurements from a Research Aircraft. *Applied Optics*, 8, 8, 1713-1732.

Turner, R. E., & Spencer, M. M., (1972). *Proceedings, Eighth International Symposium on Remote Sensing of the Environment*, Vol. II, 895-934.

Vermote, E.F., Tanré, D., Deuzé, J.L., Herman, M., & Morcrette, J.J. (1997). Second Simulation of the Satellite Signal in the Solar Spectrum, 6S: An Overview. IEEE Transactions on Geoscience and Remote Sensing, 35 (3), 675-686.

Wokocha C.C., & Omenihu E.R. (2015). Land Resources Appraisal and Management Activities using Remote Sensing Techniques: Case Study of Akpor Town, Rivers State